Highly water-soluble orotic acid nanocrystals produced by high-energy milling

Jéssica de Cássia Zaghi Compri[1], Veni Maria Andres Felli[1], Felipe Rebello Lourenço[1], Takayuki Takatsuka[2], Nikoletta Fotaki[3], Raimar Löbenberg[4], Nádia Araci Bou-Chacra[1], Gabriel Lima Barros de Araujo[1]

[1] Department of Pharmacy, Faculty of Pharmaceutical Sciences, University of São Paulo, São Paulo, Brazil

[2] Thinky Corporation, Tokyo, Japan

[3] Department of Pharmacy & Pharmacology, University of Bath, Bath, England

[4] Faculty of Pharmacy and Pharmaceutical Sciences, University of Alberta, Edmonton, Canada

Abstract

Orotic acid, a heterocyclic compound also known as vitamin B13, has shown potent antimalarial and cardiac protection activities, however, its limited water solubility has posed a barrier to its use in therapeutic approaches. Aiming to overcome this drawback, three orotic acid freeze-dried nanocrystal formulations (FA, FB and FC) were developed by using the high-energy milling method. Polysorbate 80 (FA) and povacoat® (FC) were used alone and combined (FB) as stabilizers. Nanocrystals were fully characterized by dynamic light scattering (DLS), laser diffraction (LD), transmission electron microscopy, thermal analysis (TG/DTG and DSC) and X-ray powder diffraction (XRD) revealing an acceptable polydispersity index, changes in the crystalline state with hydrate formation and z-average of 100-200nm, a remarkable 200-time reduction compare to the orotic acid raw material (44.3µm). Furthermore, saturation solubility study showed an improvement of 13 times higher than the micronized powder. In addition, cytotoxicity assay revealed mild toxicity for the FB and FC formulations prepared with povacoat®. Orotic acid nanocrystal platform can deliver innovative products allowing untapped this versatile potential of this drug substance candidate.

Keywords

Nanotechnology; Nanocrystals; Physical characterization; Physicochemical; Solubility; Formulation; Stability; Polymers; Surfactants; Stabilization.

Introduction

Orotic acid is a heterocyclic compound, whose structure, functions and potential pharmacologic actions have been studied for many years. This compound, also named vitamin B13, is produced by the human intestinal flora and it is found in many biological processes. It actively participates in the urea cycle and it is one of the precursors in pathway synthesis *de novo* of pyrimidines for replication of DNA and RNA. [1,2]

One of the most relevant pharmacological findings is its antimalarial action. Orotic acid derivatives can inhibit the activity of two key enzymes in Plasmodium replication within the host: dihydroorotase and dihydroorotate dehydrogenase [3] showing a desirable selective toxicity. The parasite dies from pyrimidine deficiency, while the patient is able to maintain their pyrimidine synthesis of uridine and cytidine nucleotides.[4]

Furthermore, studies in animals have shown that orotic acid can provide cardiac protection, contributing to the prevention of myocardium degeneracy and heart failure in animals with genetic cardiomyopathies.[5] Additionally, some researchers revealed the use of orotic acid as a food supplement for high-performance athletes. Its effects occur during physical activities by improving and maintaining ATP levels in glucose uptake. This increases the formation of ribose and muscle carnosine storage, supporting and strengthening muscle hypertrophy and increasing the contractile capacity of muscle.[6,7,8] In the cosmetic area, it presents a moisturizing

effect on skin, with an effect comparable to excipients with highly moisturizing properties, such as the pyrrolidone carboxylic acid (PCA).

Although orotic acid presents potential therapeutic properties, its aromatic nature, characterized by the presence of a pyrimidine ring confers low-water solubility to the molecule in the physiological pH range.[9] Aiming to overcome this limitation, the development of orotic acid synthetic derivatives with improved solubility has been explored as an alternative approach. These modifications take advantage of its multidentate structure by adding substituents in its pyrimidine ring, in the heterocyclic nitrogen atoms in the carboxylic oxygens, as well as in the carboxylic group.[10] However, the efficacy of these compounds remains unknown.

Recent advances in drug delivery systems can overcome this solubility problem, while maintaining the drug safety profile, such as the use of nanotechnologies. Among these, nanocrystal drugs are one of the most effective approaches. [11,12] Nanocrystals are defined as nanometer-sized particles produced from pure drugs, which are usually stabilized by surfactants and/or polymeric steric stabilizers present in the dispersion medium. In addition, they are obtained in a liquid dispersion, called nanosuspension.[13, 14,15] They have been present in the pharmaceutical market since the 2000s, when Rapamune® (immunosuppressant) was launched. Ever since, they have been one of the most promising nanostructures, due to their high earnings and low time-to-market character. By 2017 the FDA has received more than 80 applications for nanocrystal drug products.[16] Nowadays nanocrystals comprise a list of at least 17 products on market such as Emend® (prevention of chemotherapy-induced nausea and vomiting), Tricor® (cholesterol-lowering drug), Triglide® (lipid regulation), Avinza® (phychostimulant), Ritalin LA® (central nervous system stimulant), Zanaflex® (muscle relaxant), Megace® (improvement of appetite and increase in body weight in patients with cancer-associated anorexia) and Naprelan® (anti-inflammatory). [11,13,17,18] To the best of our knowledge, there is no orotic acid nanocrystal reported in the literature. [19, 15]

Different technologies were developed to obtain nanocrystals. In general, the processes are classified into two categories, top-down and bottom-up. [20,21] Among these technologies, high energy milling, a top-down method, is impressive due to several advantages, such as the short time required in the process and the simplicity in development and in the scaled-up production. [22,23,24] Despite these numerous advantages, the additional free energy of the new surfaces generated by the milling need to be compensated to avoid instability, which can be achieved by the use of proper stabilizers. [19,20,21] As the selection of stabilizers is often drug-specific, the search for new and more efficient stabilization systems is needed. [25,26] Recently, Povacoat®, a polyvinyl alcohol co-polymer derivative, has been pointed out as a promising new stabilizer for nanocrystal formulations. [27,28] In the present study, we report the beneficial effects of the use of this co-polymer and a new combination with polysorbate 80, one of the most popular stabilizers, for the development and cytotoxicity evaluation of orotic acid nanocrystals.

Experimental section

Materials

Orotic acid (OA) anhydrous (purity 99.8%) (Figure 1) was purchased from Sigma Aldrich (São Paulo, Brazil). Methylcellulose, polysorbate 80, methylparaben and glucose were obtained from Shin-Etsu (Tokyo, Japan). Povacoat® Type F (Polyvinyl alcohol/ Acrylic acid/ Methyl methacrylate copolymer) was donated from Daido Chemical Corporation (Osaka, Japan). Hydrochloric acid, sodium chloride, sodium citrate, sodium acetate, potassium phosphate monobasic, and sodium hydroxide were obtained from Synth (Sao Paulo, Brazil). Purified water was obtained from a Milli-Q Millipore water system (São Paulo, Brazil). The cell line NCTC clone 929 was donated from the Culture Section of the Cell Institute Adolfo Lutz (São Paulo, Brazil). The culture media was purchased from Interlab (São Paulo, Brazil).

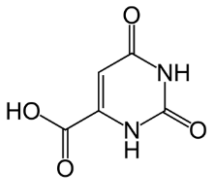

Figure 1. Molecular structure of orotic acid.

Methods

Preparation of orotic acid nanocrystals

Orotic acid nanocrystals were prepared using a rotation revolution nanopulverizer NP-100 (Tokyo, Japan) according to the method proposed by Takatsuka et al. [22]. Prior to the nanopulverization, a dispersion medium was prepared by dissolving the following stabilizers: methylcellulose (0.3% w/v), povacoat® (10% w/v) and polysorbate 80 (0.1% w/v) in the water. Three formulations were prepared using polysorbate 80 (FA), polysorbate 80 and povacoat® together (FB) and povacoat® (FC). The concentration of the orotic acid was maintained constant at 10% (w/v).

The nanopulverization was performed in two steps. In the first step, 10 g of orotic acid and 50g of the aqueous solution containing the stabilizers were transferred to the mixing vessel. A total of 35g of yttrium-stabilized zirconia milling beads with a diameter of 0.1 mm were added to the same container. At this stage, the conditions for pulverization were 1,500 rpm for 15 minutes. For the second step, 50g of aqueous solution containing the stabilizers were added to the vessel and the conditions applied were 400 rpm for 1 minute.

From the nanosuspensions obtained, an amount of 10 g was immediately freeze dried (Christ Alpha 1-5, Christ Martin, Germany) at -70°C for 48 hours under pressure of 0.120 mbar and 24 ° C using glucose (up to 5g) to prevent aggregation.

Characterization of orotic acid nanocrystals

Process efficacy and influence of the stabilizer on particle size and zeta potential and stability

Orotic acid particle size distribution was measured using laser diffraction (LD) technique (Mastersizer 2000, Malvern Instruments, England) with a small volume dispersing unit (Hydro 2000uP, Malvern Instruments, England). Samples were diluted 20-fold using Ultrapure Milli-Q® water. The nanocrystals z-average was measured by dynamic light scattering (DLS) technique using a Zetasizer Nano ZS device (Malvern Instruments, England). The samples were diluted in Milli-Q® in the ratio of 1:400 (nanocrystal:water). Measurements were performed in triplicate using a measurement angle of 90°.

The zeta potential was determined employing a Zetasizer Nano ZS 90 device (Malvern Instruments, Malvern, UK). Samples (n=3) were prepared using 20µl of a diluted nanosuspension in 4 mL of Milli-Q® water. The conductivity of the dispersion was adjusted to 50 µS/cm, with NaCl solution at pH 5.5. [29]

The stability of the freeze-dried nanosuspensions, kept under refrigeration (4°C), was evaluated by monitoring the variations in particle size distribution and z-average, polydispersity index and zeta potential values, for 3 months. Data were analyzed using Minitab 17 Statistical Software® by analysis of variance (ANOVA) and regression analysis. P-values less than 0.05 were considered statistically significant. Additionally, macroscopic observations aiming to detect sediment and agglomerates in the redispersed nanosuspensions were performed monthly.

Scanning Electron Microscopy

Orotic acid raw material was analyzed using a SU-1500 scanning electron microscope (SEM) (Hitachi High-Technologies, Tokyo, Japan). Samples were measured using 15kV acceleration voltage and images were acquired using 500x magnification. The morphology and particle size of nanocrystals were observed using a transmission electronic microscopy JEM-1010 with 80 kV (Jeol USA). Samples were obtained from a saturated solution and diluted 10x. The material was deposited on copper grids and coated with 150 MESH Formvar film for 10 minutes. In addition, Image J® Software was used for the crystal size confirmation. The analysis was performed individually for orotic acid raw material, FA, FB and FC, for which 30 crystals were measured per sample (n = 30).

Thermal analysis

Differential scanning calorimetry (DSC) curves were obtained in a DSC 7020 (Exstar, Japan). About 2 mg of samples (pure materials, physical mixture, and nanocrystals) were placed in an aluminum sample holder hermetically sealed and subjected to analysis. Dynamic N_2 atmosphere (50 mL min^{-1}) and a heating rate of 5°C min^{-1} in the temperature range of 25 to 300°C were used. The temperature range and enthalpy response were previously calibrated using an indium standard.

Thermogravimetry and derivative thermogravimetry (TG/DTG) curves were obtained using a TG / DTA 7200 (Exstar, Japan), with sample weight of approximately 5mg (platinum crucible) at a heating rate of 5°C min^{-1}, under dynamic N_2 atmosphere (100 mL min^{-1}) in the temperature range 25 to 600°C. The instrument calibration was verified employing calcium oxalate standard.

X-ray diffraction

A Bruker Diffractometer Model D8 Advance Da Vinci (Bruker, Japan) was used to characterize the solid crystalline state. Samples of the physical mixture in absolute values and nanocrystals were exposed to Cu Ka radiation 40 Kv. Measurements were performed at a scanning speed of 0.5°/min over a 2θ range of 0.01–40°.

Determination of saturation solubility

The saturation solubility of FA, FB and FC was determined by Shake-Flask method. [30] The media were determined in an exploratory experiment where orotic acid showed more solubility in media acetate pH 4.5 and water. The formulations were added to vials containing 10 mL media. After reaching saturation, the vials were properly sealed and transferred to a shaker, 430-RDBPE model (New Ethics, São Paulo, Brazil) at 37° C for 72 hours. At the end of that period, aliquots were collected; filtered using a porous micron Full-Flow 45µm filter (Millex GM, Millipore, Massachusetts, USA) and the solubilized amount of orotic acid was determined by spectrophotometric method.

Determination of orotic acid content

Orotic acid content in the nanosuspension was determined by UV spectrophotometry using an Evolution™ 201 UV-Visible Spectrophotometers (Thermo Scientific, São Paulo, Brazil)

and wavelength of 274nm. The method was developed and validated in the parameters of specificity, linearity, accuracy and precision.

Cytotoxicity

Cell line NCTC clone 929 (mouse connective tissue) CCIAL020, grown in minimal medium Eagle (MEM) supplemented with 0.1 mM non-essential amino acids, 1.0 mM sodium pyruvate and 10% fetal bovine serum without antibiotic was used in the agar diffusion method. [31,32] Samples were tested in four replicates on separate plates; for the positive controls, latex fragments (toxic) were used (0.5cm x 0.5cm); and negative controls were filter paper discs, respecting the dimensions of 0.5 cm in diameter. Samples were analyzed macroscopically observing the presence or absence of a clear halo in or around the test sample. The diameters of these halos, when present, were accurately measured, using a calibrated pachymeter. The average of the readings of halo diameters of four plates was calculated.

Results and Discussion

Process efficacy and influence of the stabilizer on particle size and zeta potential and stability

The z-average, the polydispersity index (PDI) and zeta potential (ZP) of FA, FB and FC were obtained immediately after preparation. The mean particle size values of nanocrystals were 116± 5nm (FA), 115± 6nm (FB) and 120± 6nm (FC). PDI was 0.170; 0.162; 0.188 and the ZP was-28.2±5.7mV, -3.2±7.2mV and -2.2±6.1mV, respectively for FA, FB and FC. The weight mean volume D[4.3] of the OA raw material determined by LD was 26.1µm. The surface weighted mean D[3.2] was 18.5 µm and the PDI value was 0.424. Additionally, the diameter at 10, 50 and 90% of the cumulative population distribution were d0.1=11.7 µm, d0.5=23.9 µm and d0.9=44.3 µm. Comparing with FA, FB and FC, the reduction in particle size was more than 200 times in all formulations (raw material d0.5=23.9 µm; (FA)116± 5nm, (FB)115± 6nm and (FC)120±6nm. These results indicate a highly effective performance of the high energy milling method of producing orotic acid nanocrystals. As examples for comparisons, Takatsuka et al. [22] prepared nanocrystals of 5 poorly water-soluble compounds (BCS class II and IV) by high-energy milling. The most notable reduction was obtained for nifedipine with the particle size reduction of d0.5 in 105 times (d0.5=14.6mm to 139nm). Similarly, Barbosa et al. [17] obtained furosemide nanocrystals by the same method reducing the d0.5 about 29 times from particles of 3.6µm down to d0.5 of 122nm.

The stability study was performed using the dry formulation storage in glass vessel at 4°C. The z-average, PDI and ZP values obtained during the 3 months in the stability test are presented in Figure 1. After 3 months, the values obtained were 182±5nm, 116±5nm and 117±4nm, demonstrating that only the formulation without povacoat® (FA) presented an increase in z-average over the period of three months. Povacoat® (Figure 2) is a new aqueous PVA copolymer which has demonstrated potential to effectively prevent the aggregation of nanoparticles of poorly water-soluble compounds. The main advantages of using polymers instead of conventional stabilizers as Polysorbates comprises the potential to minimize the molecular motion of the dispersed drug in the solution, prevent the crystal growth and nucleation of the dissolved drug, maintaining the supersaturation level for a long period of time and improve the storage stability by inhibiting the recrystallization of amorphous drug. In addition, Povacoat® exhibit both hydrophobic and hydrophilic properties, so the surface of a poorly water-soluble compound can be properly wetted and then sterically stabilized in a liquid medium. [27,28] The low ZP values observed in the Povacoat® formulations (FB and FC) indicate a sterically-stabilized system, what possibly compensate the free energy of the new surfaces created and help to avoid agglomeration, nucleation and crystal growth, however, the main stabilization mechanisms are still unclear and further investigation is needed to develop better and more rational screening strategies. Additionally, the PDI of FA was increased to 0.452,

while for FB and FC there were no significant changes in the PDI values. Values higher than 0.500 are related to the Ostwald ripening, being considered critical in the formulation. [33, 34]

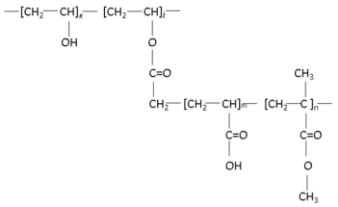

Figure 2. The chemical structure of water-soluble polymer povacoat® type F.

ZP analysis is based on the assessment of the movement of the particles in an electric field, being a fundamental parameter in the prediction of long-term stability. At the end of the third month, ZP values were -30.3±8.4mV, -4.7±7.5mV and -9.8±7.2mV, respectively for FA, FB and FC. A zeta potential of at least -30mV, for electrostatic and -20 mV for sterically stabilized systems is desired to obtain a physically stable nanosuspension.[35] However, there is no general rule. [36,37,38,39] ZP values are dependent on the type, size, molecular weight and other stabilizer characteristics. Müller et al [39] established the ZP value of polysorbate alone (-13 mV) and posteriorly this value in a very sterically-stabilized system (-3 mV). The authors observed that ZP values lower than -30 mV and -20 mV can be observed without breakage in the system. By contrast, the use of polysorbate was reported as critical for long-term stability due to its relatively thin adsorbed layer in the nanoparticles.[38,40] In summary, the feasibility of its use should be monitored case-by-case. In the present study aiming to provide effective steric stabilization, different classes of stabilizers were used: a non-ionic surfactant (polysorbate 80), a semisynthetic non-ionic polymer (methylcellulose), and a polymer (povacoat®). Their influence on the stability was statistically evaluated.

Additionally, both formulations were easily resdispersed with water during this period. In contrast, FA was challenging to redisperse in water, after liophylization, possibly due to the irreversible nanocrystal aggregation.

The results from the stability study were evaluated using ANOVA, a parametric method, which is a reliable and powerful in detecting differences in quantitative data. In ANOVA analysis, values of a significance level (p-values) less than 0.05 ($\alpha = 0.05$) indicate statistically significant models. [41] Thus, ANOVA was used as a statistical tool to evaluate the interaction among storage time, povacoat® and polysorbate 80, on z-average, ZP and PDI. For z-average (Figure 3a), povacoat® and storage time presented p-values <0.05, 0.008 and 0.02, respectively. For ZP (Figure 3b), povacoat®, polysorbate 80 and time presented p-values of 0.001, 0,440 and 0.066. For PDI (Figure 3c), p-values were 0.012 for povacoat® and time. In summary, these analyses showed that povacoat® and the storage time influenced the stability of the nanocrystals. The analysis also revealed that the total absence of this polymer was the determining factor for increasing the z-average and PDI values. A similar advantage of this polymer was identified by Yuminoki et al. [42] to stabilize Griseofulvin, Probucol, Tolbutamide and Hydrochlorothiazide nanocrystals by using high-energy milling. The author found povacoat® was the most effective in preventing nanocrystal aggregation compared to hydroxypropylcellulose (HPC), and polyvinylpyrrolidone (PVP).

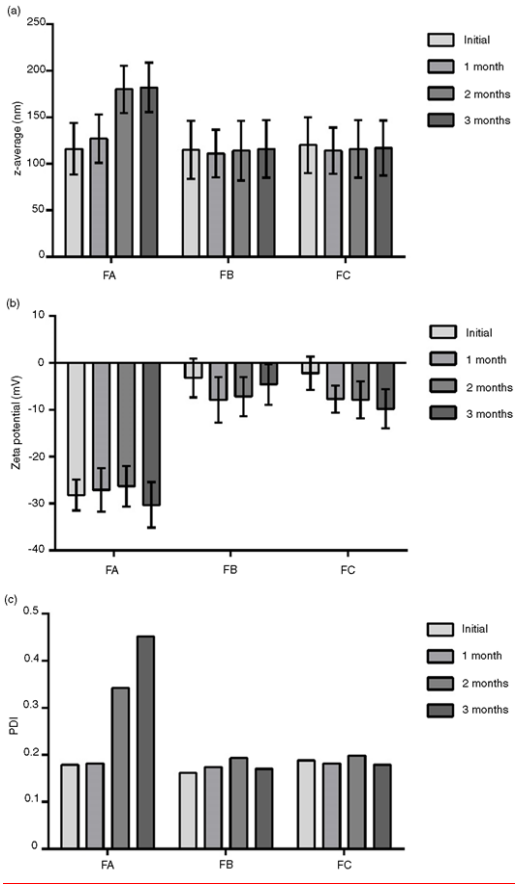

Figure 3. (a) Z-average, (b) zeta potential and (c) polydispersity index of FA, FB and FC for three months.

SEM analysis

One of the main advantages of using microscopy techniques in characterizing nanocrystal is to reveal its size independent of the particle shape. Keck [43] pointed out a critical shortcoming of these traditional measurement techniques. According to the author, DLS and DL techniques assume sphere-shaped particles for the measurement of the z-average and particle size distribution, respectively. In general, nanocrystals rarely present a sphere shape. Thus, the particle size obtained is estimated, demonstrating the importance of using a supplementary technique to overcome this limitation.[44]

Microscopy images (Figure 4) revealed differences in size, surface, and shape of OA raw material (Figure 4a) compared to nanocrystals (Figure 4b, 4c and 4d). Additionally, they revealed the presence of clusters of OA raw material (Figure 4a), which confirms the results obtained previously by DLS and DL (PDI 0.424). For FA, although PDI was 0.179±0.05 using the DLS technique, microscopy images showed aggregation (Figure 4b). Moreover, it is possible to observe the effectiveness of the milling process in the reduction of the particle size (Figure 4b, 4c and 4d). The Image J software allowed determining the crystal particle size, being 354±45nm, 141±22nm and 116±26nm respectively for FA, FB and FC (n=30). Due to the diversity in shape and size that nanocrystals can present, software such as Image J are being widely used to certify these parameters, even when the traditional methods (DLS and DL) are used. [45- 49]

Orotic acid nanocrystals apparently presented a needle-shape for all formulations. Nanocrystal shape is a distinct parameter of each substance and is closely related to the type of

vessel, centrifugal force, running time and specific characteristics of the zirconia balls used during the milling process. [22]

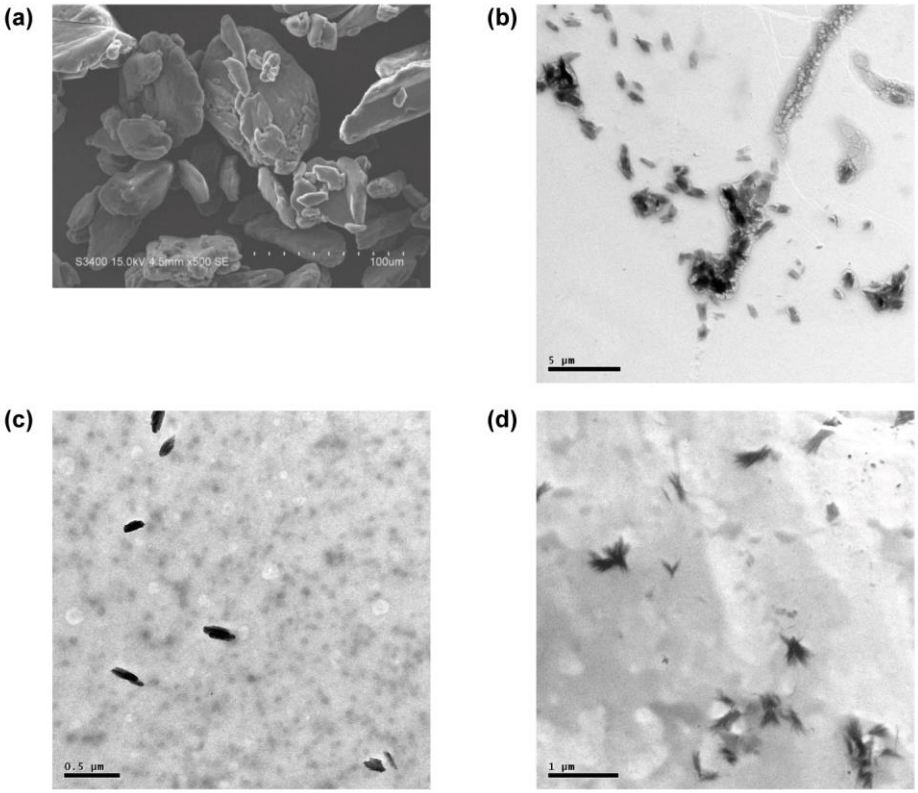

Figure 4. Images of OA raw material (a), FA (b), FB (c) and FC (d).

Thermal analysis

Thermal properties of OA raw material and FA, FB and FC were evaluated by DSC (Figures 5a, 5d and 5g respectively), TG (Figures 5b, 5e and 5h) and DTG (Figures 5c, 5f and 5i) analysis. TG profile of OA indicates the presence of two main events during the mass loss. The first event occurs between 100 and 150 °C and corresponds to the sample dehydration, suggesting that the anhydrous OA probably was converted into a hydrate during transport or storage. According to Braun et al. [50], anhydrous OA can transform into the hydrate form during storage time, depending on relative humidity of the environment. Also, a second step assigned to sublimation occurs at 330 °C, corresponding to a mass loss of 99.8%, which is followed by a slow final decomposition step.

TG/DTG curve of FA (Figures 5b and 5c) exhibits the first mass loss between 50 °C and 80 °C (Δm = 2.6%; T_{peak} = 70 °C), which is assigned to dehydration. Posteriorly, five additional events with consecutive mass loss (Δm_1 = 5.4%, Δm_2 = 9.7%, Δm_3 = 17.2% and Δm_4 = 53.8%) in the range from 105 °C to 335 °C (DTG_{peak} = 105 °C, 169 °C, 256 °C and 335 °C), followed by a slow final step at 355 ºC. For FB (Figures 5e and 5f) and FC (Figures 5h and 5i), the water loss process is less pronounced and it occurs near 50 °C. Posteriorly, two additional events of mass loss are observed at 268 °C (extrapolated onset temperature = T_{onset}) and 231 °C for FB and FC, respectively. Finally, both formulations present a slow final step between 474 ºC and 482 ºC.

DSC curves confirmed most of the events observed by thermogravimetric analysis. DSC curve of FA (Figure 5a) shows a well-defined endothermic event near to 85 °C (T_{peak} = 84 ºC), confirming the presence of the OA hydrate. For FB and FC, Figures 5d and 5g, respectively, a broad endothermic event occurs gradually from 25 °C, indicating the presence of a small amount of water superficially adsorbed, i.e. not bound to the structure. These results clearly indicate structural differences and that the freeze-drying process was not efficient to remove bound water from FA formulation. A second endothermic event in the DSC FA curve corresponds to the anticipation of the melting point of glucose (T_{peak} = 143 ºC). The third endothermic event is observed at about 183 °C (T_{peak} = 183 ºC), which suggests the anticipation of glucose decomposition. In case of FB/FC, events related to povacoat® melting were characterized by endothermic events, occurring from 160 °C to 170 °C, and by exothermic recrystallization events at 170 °C and 190 °C. [51] Thereafter, an endothermic event related to the decomposition of glucose is observed near 200 °C (T_{peak} = 197 ºC), followed by povacoat® decomposition between 231°C to 237 °C (FB T_{peak} = 231 ºC, FC T_{peak} = 237 ºC).

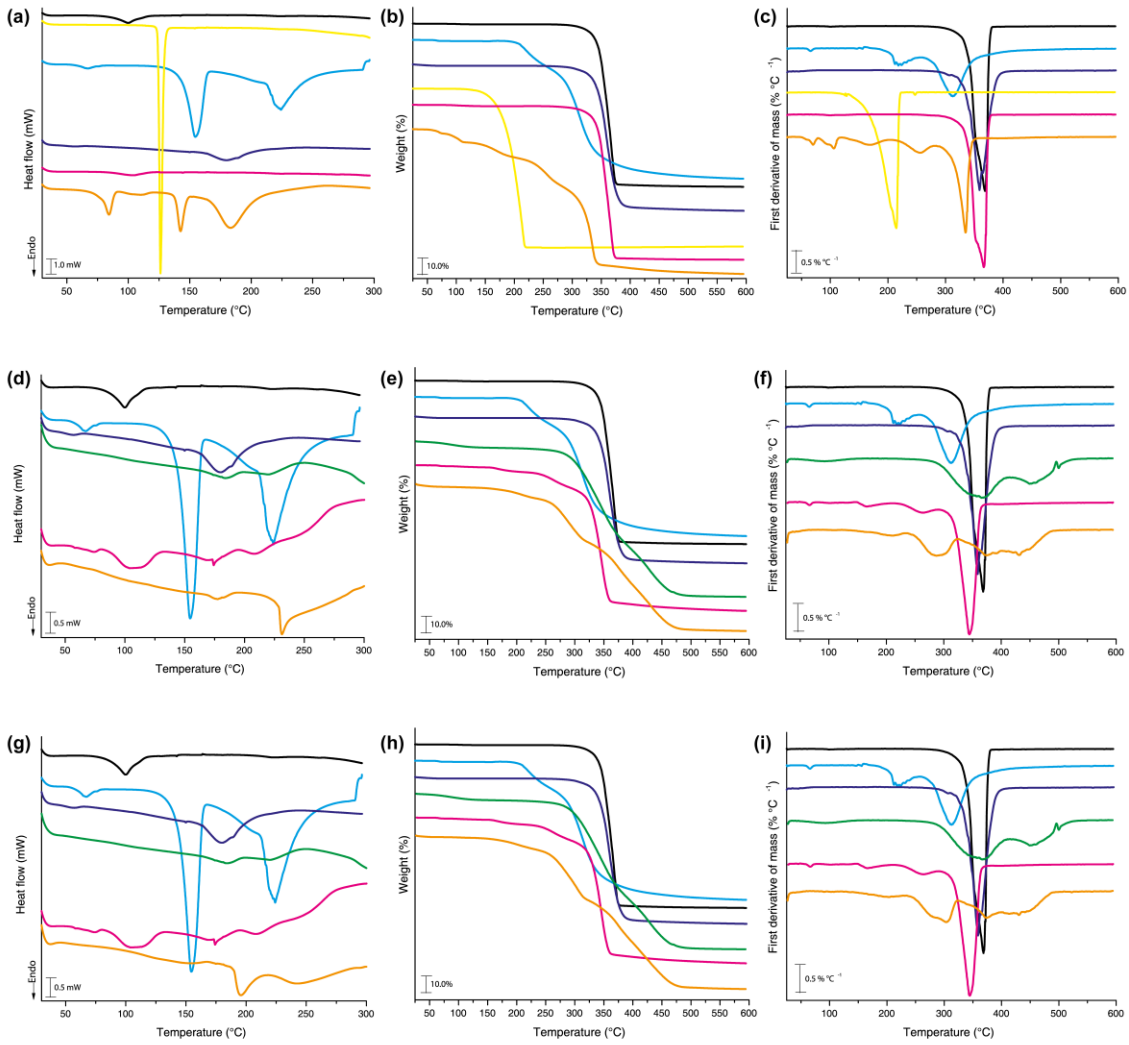

Figure 5. Thermoanalytic profiles obtained in dynamic nitrogen atmosphere (50mL min^{-1}) and heating rate 5 °C min-1: (a) DSC, (b)TG and (c) DTG curves of OA raw material, physical mixture, excipients and FA. (d) DSC, (e) TG and (f) DTG curves of OA raw material, physical mixture, excipients and FB. (g) DSC, (h)TG and (i) DTG curves of OA curves raw material, physical mixture, excipients and FC.

X-ray diffraction

The X-ray diffraction pattern of OA raw material exhibited reflections of high intensity, narrow and a well-defined boundary, indicating its crystalline nature (Figure 6). The most intense peak of OA (at 29 °) is also preserved in the formulations and physical mixture. Comparing the OA raw material with FA, FB and FC, we observed that the nanocrystals showed lower intensity in the diffraction patterns. This fact is probably caused by the significant reduction in the particle size induced by the milling process and the addition of certain degree of disorder due to amorphization and/or hydration. [50] FB and FC patterns have more similarities between them than compared to FA, in agreement with the thermal analysis results.

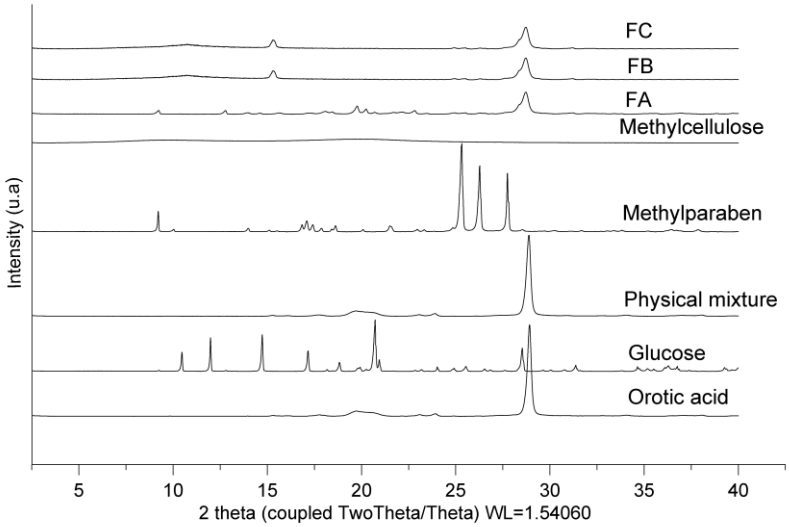

Figure 6. X-ray diffractogram of OA raw material, physical mixture, excipients and FA, FB and FC.

Determination of saturation solubility

Solubility test was performed using the media acetate pH 4.5 and water, which were selected from an exploratory solubility test on OA raw material. In these media OA presented higher saturation solubility than pH 1.2 and 6.8 and 7.2. As shown in Table 1, FA, using water, revealed the highest increase in the saturation solubility, reaching up to 13 times higher than OA raw material. FB exhibited an increase in saturation solubility up to 7.5 times higher in acetate buffer pH 4.5 compared to OA raw material. For FC, it was demonstrated that the increase in solubility was practically the same in both media: 5 times higher. Barbosa et al [17] obtained furosemide nanocrystals, using high-energy milling, with saturation solubility between 1.2 and 3.0 times higher compared to the furosemide raw material.

According to the study of the physical mixtures no enhancement in saturation solubility was observed compared to values of OA raw material (Table 1). These results confirm that the improvement in saturation solubility of nanocrystals was due to reduction of the particle size revealing innovative physical and chemical characteristics. [52] Among these nanocrystal

particularities, the most known are the increased surface area, the rise in adhesiveness and dissolution rate of poorly water-soluble drugs. These effects are elucidated by Noyes-Whitney, Kelvin and Ostwald-Freundlich equations. [53, 54, 44, 21] In general, these properties lead to improved bioavailability, provide rapid onset of action, reduction in fasted/fed state variations, [14] reduction of volume and dosages administered [55, 56] and enhanced skin delivery. [57, 58]

Additionally, some studies demonstrated that high-energy milling was the most effective method for preparing oral suspensions for pharmacological, pharmacokinetic, and safety studies on animals during the drug discovery and preclinical phase. Furthermore, it has enough potential to warrant expanding research into a new approach for preparing extemporaneous formulations for the first-in-human and early clinical studies of a candidate drug. [22]

Table 1. Saturation solubility (n=3) of OA raw material, physical mixtures of FA (PM-FA), FB (PM-FB) and FC (PM-FC), nanocrystals formulations (FA, FB and FC) and the increase in solubility.

Formulation	Media (mg/mL)						Increase in solubility (times)	
	Water			Acetate pH 4.5			Water	Acetate pH 4.5
OA	0.10	0.11	0.10	0.20	0.18	0.19	RV	RV
PM- FA	0.09	0.10	0.09	0.21	0.20	0.20	-	-
PM- FB	0.11	0.11	0.10	0.22	0.21	0.21	-	-
PM- FC	0.11	0.10	0.10	0.19	0.20	0.20	-	-
FA	1.35	1.37	1.36	2.20	2.22	2.20	13.6	11.0
FB	0.65	0.66	0.63	1.50	1.48	1.51	6.3	7.5
FC	0.65	0.56	0.56	1.02	1.03	1.04	5.6	5.0

RV: reference value; - : not observed; OA: orotic acid raw material; PM-FA: physical mixtures of orotic acid, methylcellulose, polysorbate 80 and glucose; PM-FB: physical mixture of orotic acid, methylcellulose, polysorbate 80, povacoat® and glucose; PM-FC: physical mixtures of orotic acid, methylcellulose, povacoat® and glucose; FA: nanocrystal formulation FA; FB: nanocrystal formulation FB; FC: nanocrystal formulation FC.

Cytotoxicity

The agar diffusion test is a qualitative assessment of toxicity, which is used as a screening evaluation in developing process of new products due to its practicality and low cost. This method proved to be suitable for screening assays and evaluating the toxicity of new products basing themselves on their ability to predict irritation *in vivo*. In addition, it contributes significantly to reducing animal assays. [59-62] According to US Pharmacopeia, [32] the cytotoxicity of FA, FB and FC were classified by the size of cell death area on the plate. The results can be observed in Figure 7. FA (Figure 7c) presented cell death in the entire plate and its graded reactivity was Grade 4 (severe toxicity). However, both FB (Figure 7d) and FC (Figure 7e), showed average cell death area of 0.1333 cm and 0.139 cm, respectively, and were graded as Grade 2 (mild toxicity). The severe cytotoxicity shown by FA could be explained due to the high concentration of OA in formulation (42.5%). FB and FC showed mild toxicity probably due to the difference of excipients in the formulations; besides the OA content was more than 3 times lower than in FA. While the nanocrystals might be used as a primary formulation, this toxicity presented by the FA must be investigated, considering the concentration that will be used in the final product.

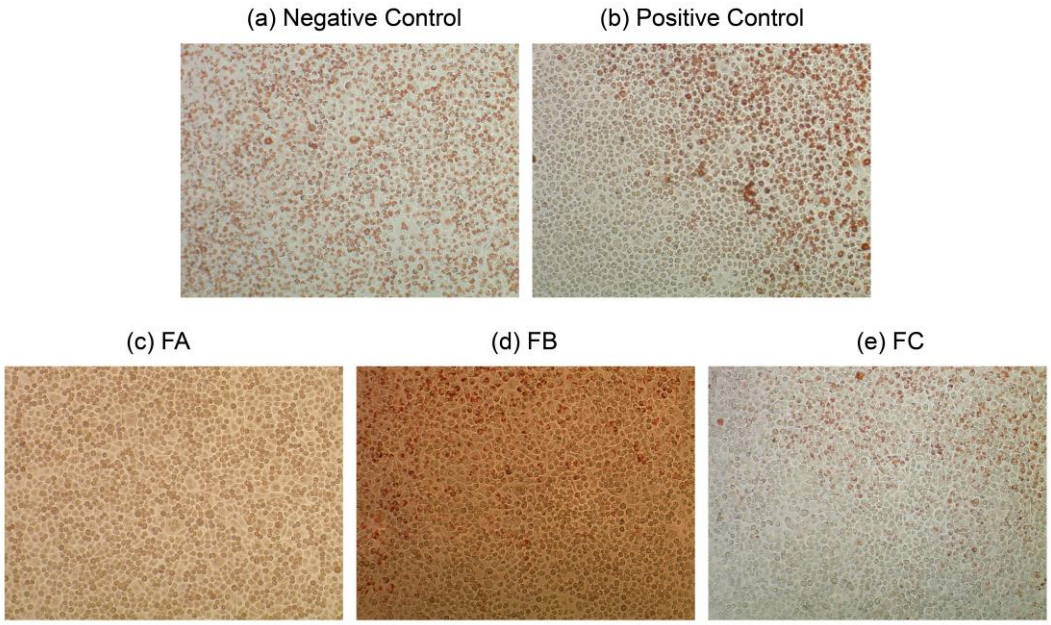

Figure 7. Images of cytotoxicity assay. Negative control (a), Positive control (b) FA (c), FB (d) and FC (e).

Conclusion

High-energy milling technique successfully allowed a particle size reduction of orotic acid to the nanosize range (100- 200 nm). The nanocrystals obtained presented a significant increase in the saturation solubility compared to orotic acid raw material, up to 13 times. Povacoat®, as stabilizer agent, provided stable formulations with improved and better physicochemical characteristics. Additionally, cytotoxicity assay revealed mild toxicity for the stable formulations which could be improved by controlling the final concentration in the formulation. Thus, orotic acid nanocrystals produced with povacoat® have the potential, as a platform, to develop unique drug products, cosmetics and food supplements.

Acknowledgements

CNpQ, FAPESP, Instituto Adolfo Lutz, Think Corporation, Daido Chemical. Jim Hesson of AcademicEnglishSolutions.com revised the English of this article.

1. Kacso I; Borodi G; Fărcaş SI; Bratu I. Inclusion compound of vitamin B13 in b-Cyclodextrin. Structural investigations. *J* Phys Conf Ser 2009;189:1-4.
2. Cuellar A, Alcolea MP, Rastogi VK., Kiefer W, Schlücker S, Rathor SK. FT-IR and FTRaman spectra of 5-fluoroorotic acid with solid state simulation by DFT methods. Spectrochim Acta A Mol Biomol Spectrosc 2014;132:430-445.
3. Krungkrai J, Krungkrai SR, Phakanont K. Antimalarial activity of orotate analogs that inhibit dihydroorotase and dihydroorotase dehydrogenase. Biochem Pharmacol 1992;43(6):1295-1301.
4. Christopherson RI, Lyons SD, Wilson PK. Inhibitors of de Novo Nucleotide Biosynthesis as Drugs. Acc Chem Res 2002;35(11): 961-971.
5. Jasmin G, Proschek L. Effect of Orotic Acid and Magnesium Orotate on the Development and Progression of the UM-X7.1 Hamster Hereditary Cardiomyopathy. Cardiovasc Drugs Ther 1998; 12 Suppl 2:189-195.
6. Rosenfeldt FL, Richards SM, Lin Z, Pepe S, Conyers RA. Mechanism of cardioprotective effect of orotic acid. Cardiovasc Drugs Ther 1998;12 Suppl 2:159-170.
7. Geiss KR, Stergiou N, Jester, Neuenfeld HU, Jester HG. Effects of magnesium orotate on exercise tolerance in patients with coronary heart disease. Cardiovasc Drugs Ther 1998;12 Suppl 2:153-156.
8. Meerson FZ, Rosanova LS. Effect of actinomycin and combination of nucleic acid synthesis activators on the development of fatigue and fitness. Doki. Akad. Nauk. SSSR 1967;166:496-499.
9. Hasunuma K, Abe T, Masahiro K. Kanebo, LTD. Cosmetic composition containing vitamin e orotate. US nº 4000276A, 24 ago. 1973, 28 dez. 1976. Available at: http://www.freepatentsonline.com/4000276.html. Accessed April 27, 2014.
10. Refat MS, Alghool S, El-Halim HFA. Alkaline earth metal (II) complexes of vitamin B13 with bidentate orotate ligands: Synthesis, structural and thermal studies. C R Chim 2010;14(5):496-502.
11. Müller RH, Keck CM. Twenty years of drug nanocrystals: Where are we, and where do we go?. Eur J Pharm Biopharm 2012;80(1):1-3.

12. Mauludin R, Muller RH. Physicochemical properties of hesperidin nanocrystal. Int J Pharm Pharm Sci 2013;5:954–960.
13. Müller RH, Gohla S, Keck CM. State of the art of nanocrystals: Special features, production, nanotoxicology aspects and intracellular delivery. Eur. J. Pharm. Biopharm 2011;78(1):1-9.
14. Gao L, Liu G, Ma J, Wang X, Zhou L, Li X, Wang F. Application of drug nanocrystal technologies on oral drug delivery of poorly soluble drugs. Pharm Res 2013; 30(2):307–324.
15. Junyaprasert VB, Morakul B. Nanocrystals for enhancement of oral bioavailability of poorly water-soluble drugs. Asian J Pharm Sci 2014; 10(1):13-23.
16. Chen ML, John M, Lee SL, Tyner KM. Development Considerations for Nanocrystal Drug Products. AAPS J 2017;19(3):642.
17. Barbosa SF, Takatsuka T, Tavares GD, Araújo GL, Wang H, Vehring R, Löbenberg R, Bou-Chacra NA. Physical–chemical properties of furosemide nanocrystals developed using rotation revolution mixer. Pharm Dev Technol 2016;21(7):812-822.
18. Jog R, Burgess DJ. Pharmaceutical Amorphous Nanoparticles. J Pharm Sci 2017;106(1):39-65.
19. Möschwitzer JP. Drug nanocrystals in the commercial pharmaceutical development process. Int J Pharm 2013;453(1):142-156.
20. Xia D, Gan Y, Cui F. Application of Precipitation Methods for the Production of Water-insoluble Drug Nanocrystals: Production Techniques and Stability of Nanocrystals. Curr Pharm Des 2014;20(3):408-435.
21. Sinha B, Müller RH, Möschwitzer JP. Bottom-up approaches for preparing drug nanocrystals: Formulations and factors affecting particle size. Int J Pharm 2013; 453(1):126-141.
22. Takatsuka T, Endo T, Jianguo Y, Yuminoki K, Hashimoto N. Nanosizing of poorly water soluble compounds using rotation revolution mixer. Chem Pharm Bull 2009;57(10):1061–1067.
23. Chen H, Chalermchai K, Xiangliang Y, Xueling C, Jinming G. Nanonization strategies for poorly water-soluble drugs. Drug Discovery Today 2011;16(7-8):354-360.

24. THINKY CORPORATION (Org.). Wet Pulverizing. Available at: http://www.thinkyusa.com/commentary/funsai.html. Accessed May 20, 2010.
25. Peltonen L, Hirvonen J. Pharmaceutical nanocrystals by nanomilling: critical process parameters, particle fracturing and stabilization methods. J Pharm and Pharmac 2010;62:1569–1579.
26. Eerdenbrugh B, Mooter G, Augustijns P. Top-down production of drug nanocrystals: Nanosuspension stabilization, miniaturization and transformation into solid products. Int J Pharm 2008;364(2008):64-75.
27. Yuminoki K, Seko F, Horii S, Takeuchi H, Teramoto K, Nakada Y, Hashimoto N. Application of povacoat as dispersion stabilizer of nanocrystal formulation. Asian J Pharm Sci 2016;11(1)48-49.
28. Yuminoki K, Seko F, Horii S, Takeuchi H, Teramoto K, Nakada Y, Hashimoto N. Preparation and Evaluation of High Dispersion Stable Nanocrystal Formulation of Poorly Water-Soluble Compounds by Using Povacoat. J Pharm Sci 2014;103(11):3772-3781.
29. Romero GB, Keck CM, Müller RH, Bou-Chacra NA. Development of cationic nanocrystals for ocular delivery. Eur J Pharm Biopharm 2016;107:215-222.
30. United States Pharmacopeia and National Formulary (USP 33-NF 28).4 Rockville, MD: United States Pharmacopeial Convention; 2010.
31. INTERNATIONAL ORGANIZATION FOR STANDARTIZATION. ISO 10993-5: Biological evaluation of medical devices. Part 5. Test of cytotoxicity: in vitro methods. Geneva: ISO, 2009:9.
32. United States Pharmacopeia and National Formulary [USP 39 NF 34]. 3 Rockville, MD: United States Pharmacopeial Convention; 2015.
33. Rabinow BE. Nanosuspensions in drug delivery. Nat Rev Drug Discov 2004;3(9):785–796.
34. Verma S, Lan Y, Gokhale R, Burgess DJ. Quality by design approach to understand the process of nanosuspension preparation. Int J Pharm 2009;371:185–198.
35. Gao L, Zhang D, Chen M. Drug nanocrystals for the formulation of poorly soluble drugs and its application as a potential drug delivery system. J Nanopart Res 2008;10(5):845.

36. Muller RH, Peters K. Nanosuspensions for the formulation of poorly soluble drugs. Preparation by a size-reduction technique. Int J Pharm 1998;160(2):229–237.
37. Tuomela A, Hirvonen J, Peltonen L. Stabilizing Agents for Drug Nanocrystals: Effect on Bioavailability. Pharmaceutics 2016;8(2):16-34.
38. Riddick, TM. Control of Colloid Stability Through Zeta Potential. Wynnewood, Pennsylvania:1st ed., Livingston Publishing Company, 1968.
39. Müller Rainer H. Colloidal Carriers for Controlled Drug Delivery and Targeting: Modification, Characterization and in Vivo Distribution. 1st ed. Stuttgart: Taylor & Francis, 1991:379.
40. Mishra PR, Al Shaal L, Müller RH, Keck CM. Production and characterization of Hesperetin nanosuspensions for dermal delivery. Int J Pharm 2009; ;371(1-2):182-189.
41. Myers RH, Montgomery DC, Anderson-cook CM. Response Surface Methodology: Process and Product Optimization Using Designed Experiments. 3. ed. Hoboken: John Wiley, 2009:704.
42. Yuminoki K, Takeda M, Kitamura K, Numata S, Kimura K, Takatsuka T, Hashimoto N. Nano-pulverization of poorly watersoluble compounds with low melting points by a rotation revolution pulverizer. Pharmazie 2012;67(8):681–686.
43. Keck CM. Particle size analysis of nanocrystals: Improved analysis method. Int J Pharm 2009;390(1):3-12.
44. Keck CM, Müller RH. Size analysis of submicron particles by laser diffractometry—90% of the published measurements are false. Int J Pharm 2007;355(1-2):150-163.
45. Choi JS, Park JS. Development of docetaxel nanocrystals surface modified with transferrin for tumor targeting. Drug Des Devel Ther 2016;11:17-26.
46. Chen F, Huang P, Zhu YJ, Wu J, Zhang CL, Cui DX. The photoluminescence, drug delivery and imaging properties of multifunctional Eu3+/Gd3+ dual-doped hydroxyapatite nanorods. Biomaterials 2011;32(34):9031-9039.
47. Teodoro JS, Simões AM, Duarte FV, Rolo AP, Murdoch RC, Hussain SM, Palmeira CM. Assessment of the toxicity of silver nanoparticles in vitro: A mitochondrial perspective. Toxicol In Vitro 2011;25(3):664-670.

48. Ma M, Huang Y, Chen H, Jia X1, Wang S, Wang Z, Shi J. Bi2S3-embedded mesoporous silica nanoparticles for efficient drug delivery and interstitial radiotherapy sensitization. Biomaterials 2015;37:447-455.
49. Sohn JS, Yoon DS, Sohn JY, Park JS, Choi JS. Development and evaluation of targeting ligands surface modified paclitaxel nanocrystals. Mater Sci Eng C Mater Biol Appl 2017;72:228-237.
50. Braun DE, Nartowski KP, Khimyak YZ, Morris KR, Byrn SR, Griesser UJ. Structural Properties, Order–Disorder Phenomena, and Phase Stability of Orotic Acid Crystal Forms. Mol Pharm 2016;13(3):1012-1029.
51. Xu M, Zhang C, Luo Y, Xu L, Tao X, Wang Y, He H, Tang X. Application and functional characterization of POVACOAT, a hydrophilic co-polymer poly(vinyl alcohol/acrylic acid/methyl methacrylate) as a hot-melt extrusion carrier. Drug Dev Ind Pharm 2014;40(1):126-135.
52. Mauludin R., Muller RH, Keck CM. Development of an oral rutin nanocrystal formulation. Int J Pharm 2009;370(1-2):202-209.
53. Noyes AA, Whitney WR. The rate of solution of solid substances in their own solutions. J Am Chem Soc 1897;19(12):930–934.
54. Buckton G, Beezer AE. The relationship between particle size and solubility. Int J Pharm 1992;82(3):7-10.
55. Rabinow B, Kipp J, Papadopoulos P, Wong J, Glosson J, Gass J, Sun CS, Wielgos T, White R, Cook C, Barker K, Wood K. Itraconazole IV nanosuspension enhances efficacy through altered pharmacokinetics in the rat. Int J Pharm 2007;339(1-2):251-260.
56. Gao L, Zhang D, Chen M. Drug nanocrystals for the formulation of poorly soluble drugs and its application as a potential drug delivery system. J Nanopart Res 2008;10(5):845.
57. Shegokar R, Muller R. NanoCrystals: industrially feasible multifunctional formulation technology for poorly soluble actives. Int J Pharm 2010;399(1-2):129–139.

58. Vidlářová L, Romero GB, Hanuš J, Štěpánek F, Müller RH. Nanocrystals for dermal penetration enhancement – Effect of concentration and underlying mechanisms using curcumin as model. Eur J Pharm Biopharm 2016;104:216-225.
59. Pinto TJA, Ikeda TI, Miyamaru LL, Bárbara MCS, Santos RP, Cruz AS. Cosmetic safety: proposal for the replacement of in vivo (Draize) by in vitro test. Open Toxicol J 2009;3:1–7.
60. Wood N, Ferguson JL, Gunaratne HQN, Seddon KR, Royston G, Stephens GM. Screening ionic liquids for use in biotransformations with whole microbial cells. Green Chem 2011;13(7):1843-1851.
61. Bauer AW, Kirby WM, Sherris JC, Turck M. Antibiotic susceptibility testing by a standardized single disk method. Am J Clin Pathol 1996;45(4):493–496.
62. Vedel G, Peyret M, Gayral JP, Millot P. Evaluation of an expert system linked to a rapid antibiotic susceptibility testing system for the detection of beta-lactam resistance phenotypes. Res Microbiol 1996;147(4):297–309